Electronic Supplementary Information for

Enhancing the energy barrier by replacing the counterions in two Holmium(III)−pentagonal bipyramidal single-ion magnets

Lei-Lei Li*, Hong-Dan Su, Shuang Liu* and Wen-Zhen Wang

School of Chemistry and Chemical Engineering, Xi'an Shiyou University, Xi'an 710065, China.
Email: lll@xsyu.edu.cn; liush@xsyu.edu.cn

Contents:

1. Crystal data and structures

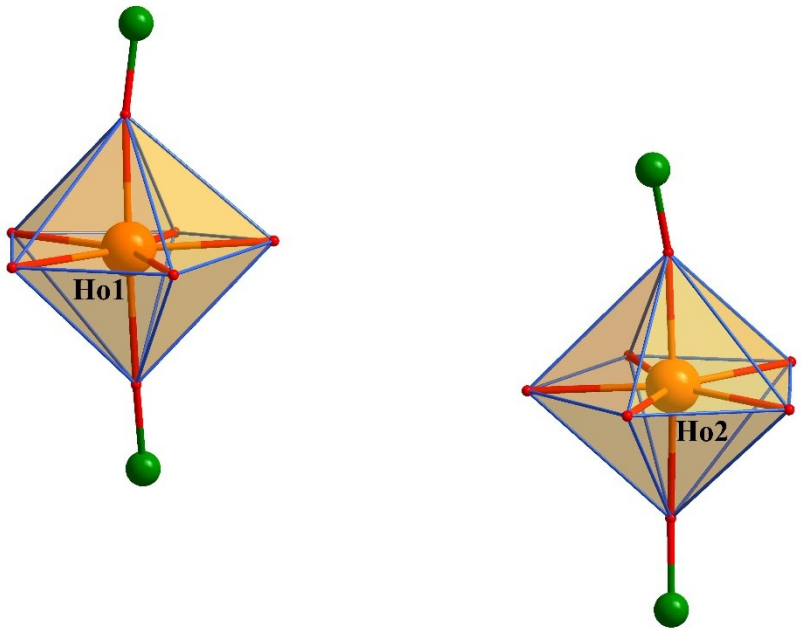

Fig S1. Coordination polyhedrons of Ho^{III} centers in **1**. Color codes: Ho orange, O red, P green.

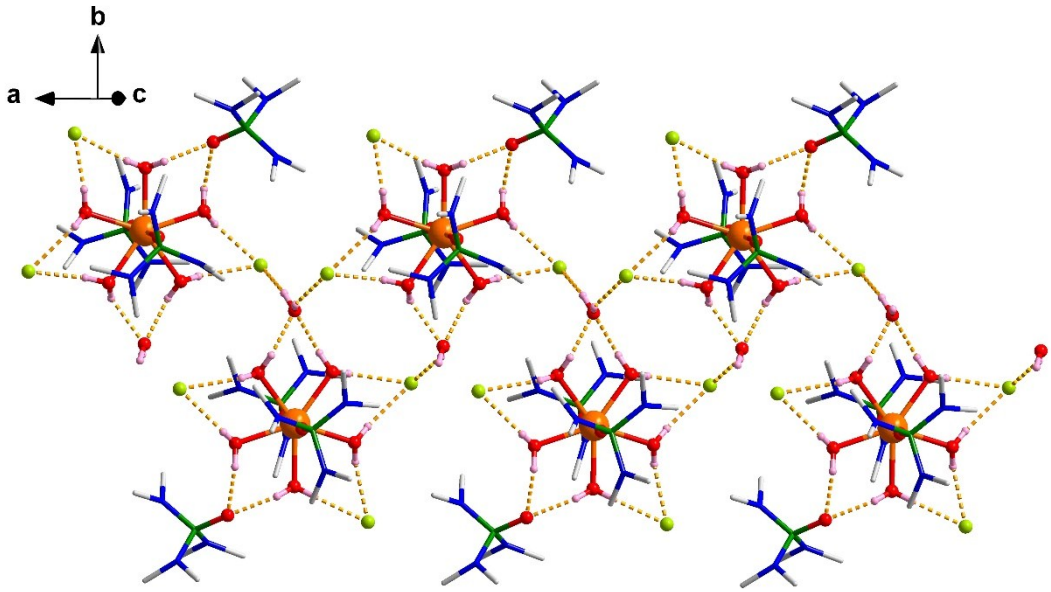

Fig S2. The 1D zig-zag chain constructed by hydrogen bonds among coordinated H_2O molecules and free solvents, free ligands and Cl^- ions in **1**. H atoms of HMPA ligands are omitted for clarity. Color codes: Ho orange, O red, H pink, N blue, C gray, P green, Cl lime. The dashed lines represent hydrogen bonds.

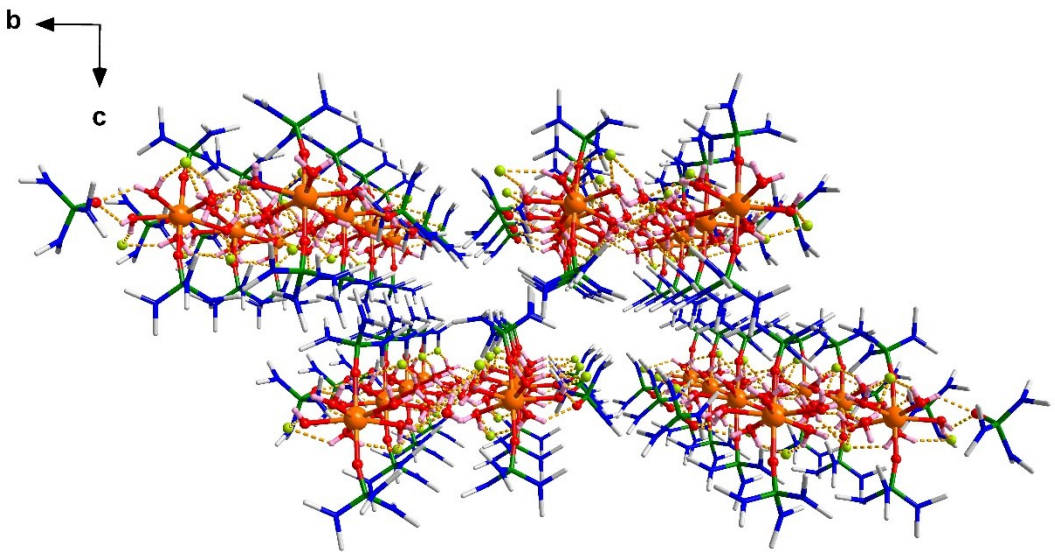

Fig S3. The 3D packing structure of **1**. H atoms of HMPA ligands are omitted for clarity. Color codes: Ho orange, O red, H pink, N blue, C gray, P green, Cl lime. The dashed lines represent hydrogen bonds.

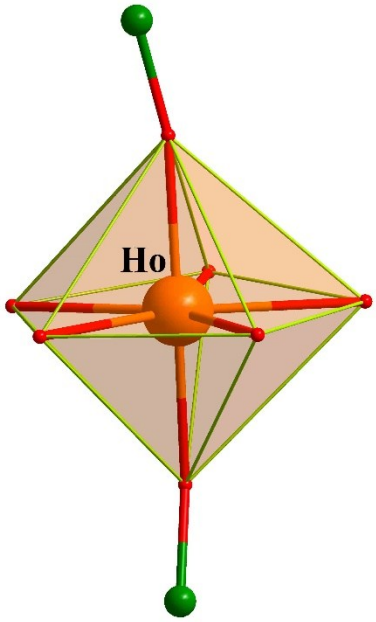

Fig S4. The coordination polyhedron of Ho^{III} center in **2**. Colour codes: Ho orange, O red, P green.

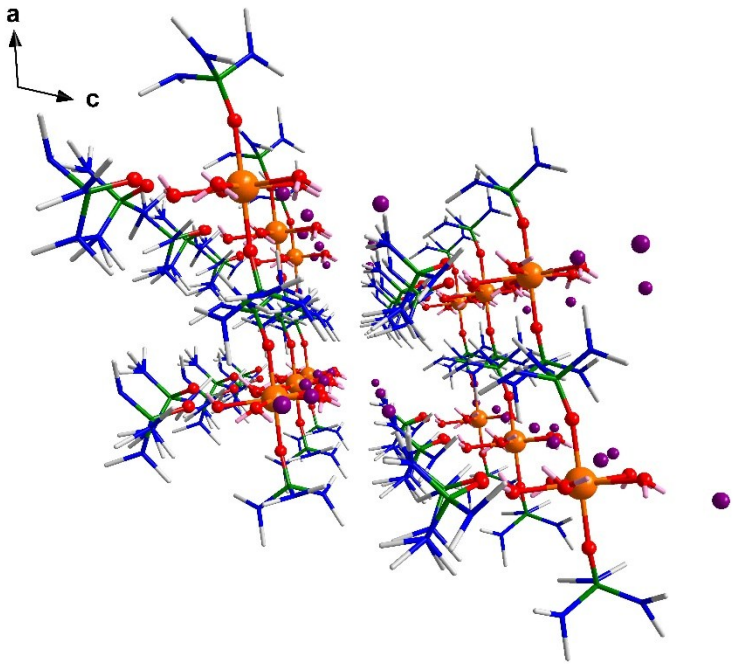

Fig S5. The 3D packing structure of **2**. H atoms of HMPA ligands are omitted for clarity. Color codes: Ho orange, O red, H pink, N blue, C gray, P green, Br violet.

Table S1. Crystallographic Data and Structure Refinement for **1** and **2**.

Compound	**1**	**2**
Formula	$C_{36}H_{132}Cl_6Ho_2N_{18}O_{18}P_6$	$C_{24}H_{82}Br_3HoN_{12}O_9P_4$
Formula weight	1833.97	1211.55
Temperature (K)	296.15	120.0(10)
Crystal system	Monoclinic	Monoclinic
Space group	$P2_1/c$	Cc
a (Å)	11.3789(9)	15.2772(6)
b (Å)	38.503(3)	15.5914(4)
c (Å)	19.9088(16)	22.7448(7)
α (°)	90	90
β (°)	101.950(2)	106.623(4)
γ (°)	90	90
V (Å^3)	8533.4(12)	5191.2(3)
Z	4	4
D_c, (g cm^{-3})	1.428	1.550
μ, (mm^{-1})	2.201	4.006
F (000)	3776	2456
GOF on F^2	1.014	0.984
R_{int}	0.0766	0.0440
$R_1{}^a$, $wR_2{}^b$ [$I > \sigma(I)$]	0.0501, 0.0954	0.0420, 0.0609
$R_1{}^a$, $wR_2{}^b$ (all data)	0.0985, 0.1145	0.0521, 0.0670
Residues (e Å^{-3})	0.63/−0.74	1.33/−0.90

[a] $R_1 = \Sigma(||F_o|-|F_c||)/\Sigma|F_o|$. [b] $wR_2 = [\Sigma w(|F_o|^2-|F_c|^2)^2/\Sigma w(F_o^2)^2]^{1/2}$

Table S2. Selected bonds and angles for complex **1**

Bonds/Angles	°/Å	Bonds/Angles	°/Å
Ho1−O4	2.348(4)	Ho2−O14	2.353(4)
Ho1−O5	2.344(4)	Ho2−O11	2.345(5)
Ho1−O7	2.331(5)	Ho2−O12	2.325(4)
Ho1−O3	2.328(4)	Ho2−O9	2.202(4)
Ho1−O1	2.197(4)	Ho2−O13	2.347(4)
Ho1−O2	2.224(4)	Ho2−O8	2.205(4)
Ho1−O6	2.332(4)	Ho2−O10	2.330(4)
O5−Ho1−O4	72.20(16)	O11−Ho2−O14	143.52(16)
O7−Ho1−O4	144.40(16)	O11−Ho2−O13	144.30(16)
O7−Ho1−O5	143.35(16)	O12−Ho2−O14	143.99(16)
O7−Ho1−O6	71.77(17)	O12−Ho2−O11	72.38(17)
O3−Ho1−O4	72.12(16)	O12−Ho2−O13	72.09(17)
O3−Ho1−O5	143.88(17)	O12−Ho2−O10	143.94(17)
O3−Ho1−O7	72.64(17)	O9−Ho2−O14	90.14(17)
O3−Ho1−O6	144.40(17)	O9−Ho2−O11	89.51(17)
O1−Ho1−O4	93.52(17)	O9−Ho2−O12	93.81(17)
O1−Ho1−O5	88.13(17)	O9−Ho2−O13	89.47(17)
O1−Ho1−O7	90.50(17)	O9−Ho2−O8	176.63(17)
O1−Ho1−O3	88.64(18)	O9−Ho2−O10	89.31(17)
O1−Ho1−O2	178.12(18)	O13−Ho2−O14	72.17(16)
O1−Ho1−O6	91.31(17)	O8−Ho2−O14	86.89(16)
O2−Ho1−O4	86.31(16)	O8−Ho2−O11	91.92(17)
O2−Ho1−O5	90.04(16)	O8−Ho2−O12	89.53(17)
O2−Ho1−O7	90.72(17)	O8−Ho2−O13	91.14(17)
O2−Ho1−O3	93.08(17)	O8−Ho2−O10	88.24(16)
O2−Ho1−O6	87.73(17)	O10−Ho2−O14	71.78(16)
O6−Ho1−O4	143.32(17)	O10−Ho2−O11	71.73(17)
O6−Ho1−O5	71.65(17)	O10−Ho2−O13	143.93(17)

Table S3. Selected bonds and angles for complex **2**

Bonds/Angles	°/Å	Bonds/Angles	°/Å
Ho1−−O19	2.222(7)	O19−Ho1−O29	91.0(2)
Ho1−−O22	2.203(6)	O19−Ho1−O32	88.5(3)
Ho1−−O29	2.354(6)	O19−Ho1−O58	89.1(3)
Ho1−−O32	2.338(7)	O19−Ho1−O70	91.5(3)
Ho1−−O58	2.353(7)	O19−Ho1−O76	89.0(3)
Ho1−−O70	2.353(7)	O22−Ho1−O19	179.2(3)
Ho1−−O76	2.344(7)	O22−Ho1−O29	88.6(2)
O22−Ho1−O58	91.4(3)	O22−Ho1−O32	90.7(3)
O22−Ho1−O70	89.2(3)	O32−Ho1−O70	144.0(2)
O22−Ho1−O76	90.9(2)	O32−Ho1−O76	72.4(3)
O32−Ho1−O29	71.5(3)	O58−Ho1−O29	70.8(3)
O32−Ho1−O58	142.2(2)	O58−Ho1−O70	73.8(3)
O76−Ho1−O29	143.9(3)	O70−Ho1−O29	144.5(3)
O76−Ho1−O58	145.3(3)	O76−Ho1−O70	71.5(2)

Table S4. Continuous Shape Measures (*CShM*)[1] calculation for complex **1**

Structure	HP-7	HPY-7	PBPY-7	COC-7	CTPR-7	JPBY-7	JETPY-7
Ho1	34.417	25.678	0.154	7.408	5.618	2.846	23.880
Ho2	34.496	25.281	0.127	7.566	5.852	2.733	24.624

HP-7 = Heptagon (D_{7h}); HPY-7 = Hexagonal pyramid (C_{6v}); PBPY-7 = Pentagonal bipyramid (D_{5h}); COC-7 = Capped octahedron (C_{3v}); CTPR-7 = Capped trigonal prism (C_{2v}); JPBPY-7 = Johnson pentagonal bipyramid J13 (D_{5h}); JETPY-7 = Johnson elongated triangular pyramid J7 (C_{3v}). Smaller value means closer to the ideal configuration.

Table S5. Continuous Shape Measures (*CShM*)[1] calculation for complex **2**

Structure	HP-7	HPY-7	PBPY-7	COC-7	CTPR-7	JPBY-7	JETPY-7
Ho1	34.341	25.815	0.105	7.956	6.130	2.727	24.524

HP-7 = Heptagon (D_{7h}); HPY-7 = Hexagonal pyramid (C_{6v}); PBPY-7 = Pentagonal bipyramid (D_{5h}); COC-7 = Capped octahedron (C_{3v}); CTPR-7 = Capped trigonal prism (C_{2v}); JPBPY-7 = Johnson pentagonal bipyramid J13 (D_{5h}); JETPY-7 = Johnson elongated triangular pyramid J7 (C_{3v}). Smaller value means closer to the ideal configuration.

2. PXRD patterns

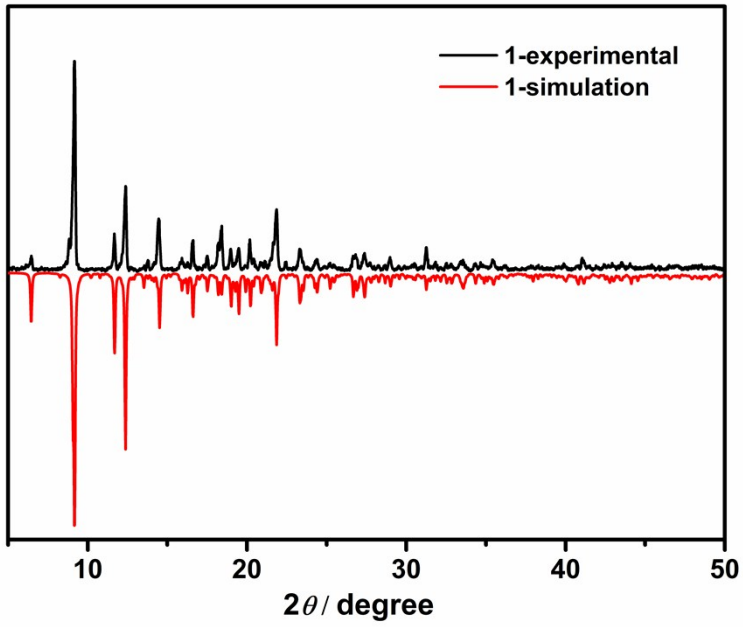

Fig S6. The powder X-ray diffraction pattern for **1**.

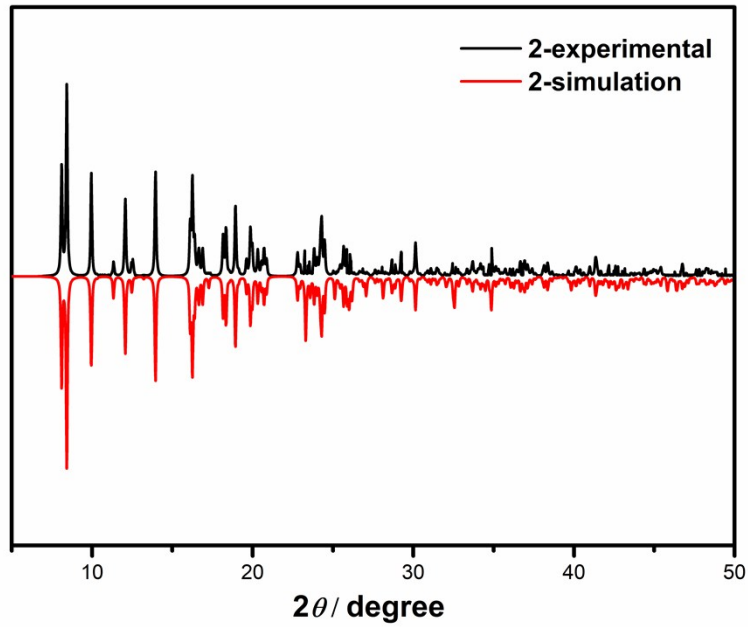

Fig S7. The powder X-ray diffraction pattern for **2**.

3. Other magnetic data

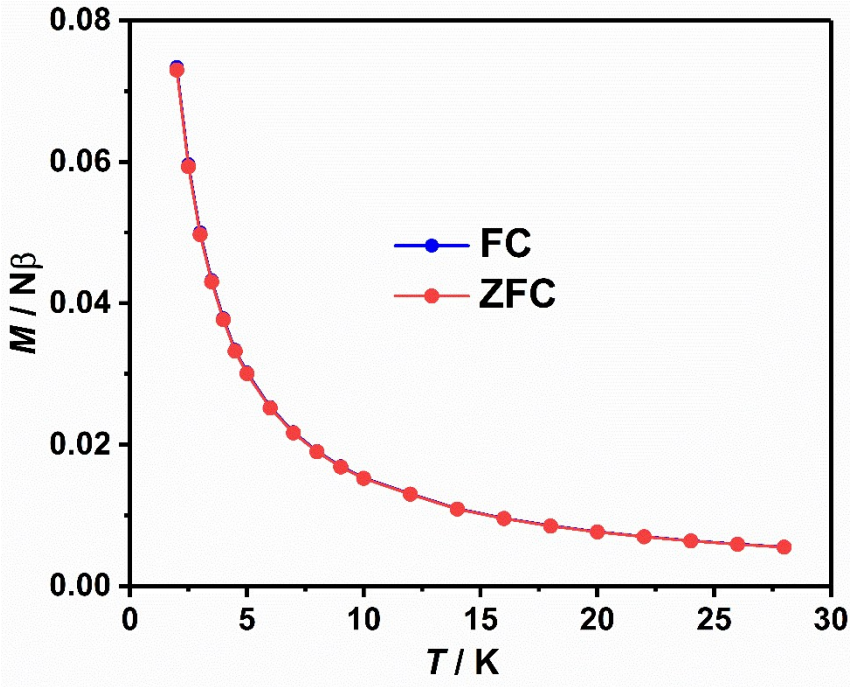

Fig S8. The zero-field cooling (ZFC) and field cooling (FC) curves for **1**. The FC data was collected in cooling mode. The temperature changing rate is *ca*. 0.008 K/s.

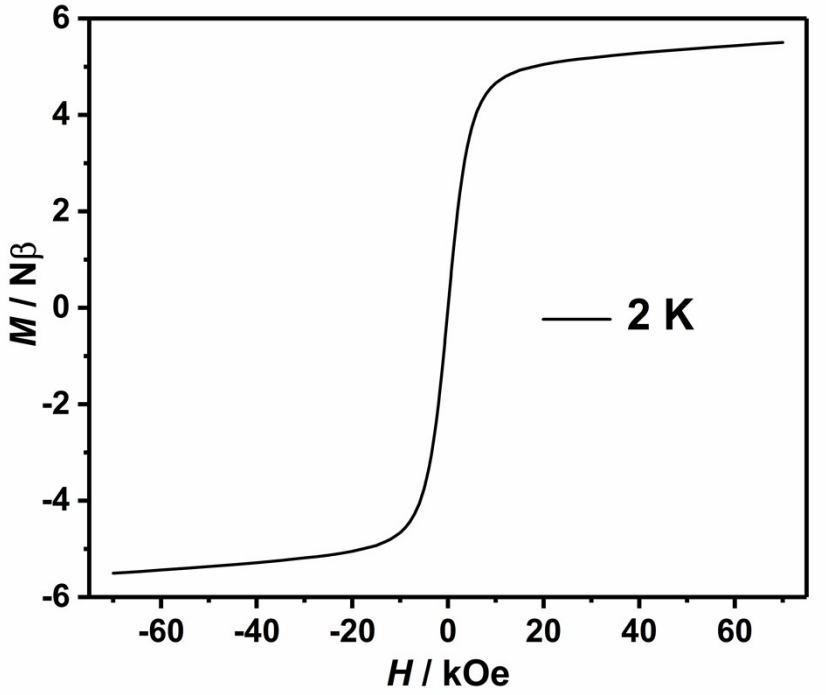

Fig S9. The hysteresis loop with the field sweeping rate of 200 Oe·s^{-1} for **1**.

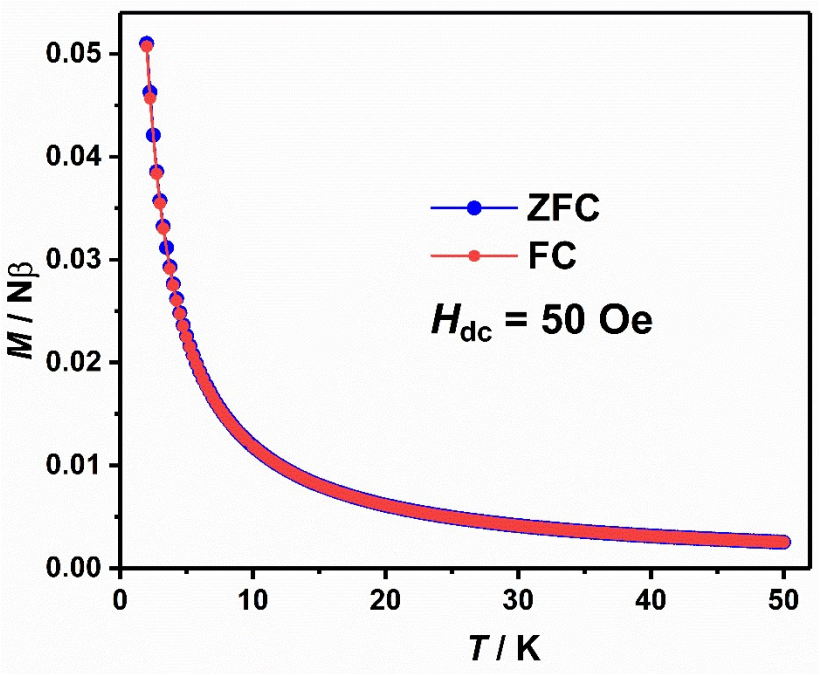

Fig S10. The zero-field cooling (ZFC) and field cooling (FC) curves for **2**. The FC data was collected in cooling mode. The temperature changing rate is *ca*. 0.008 K/s.

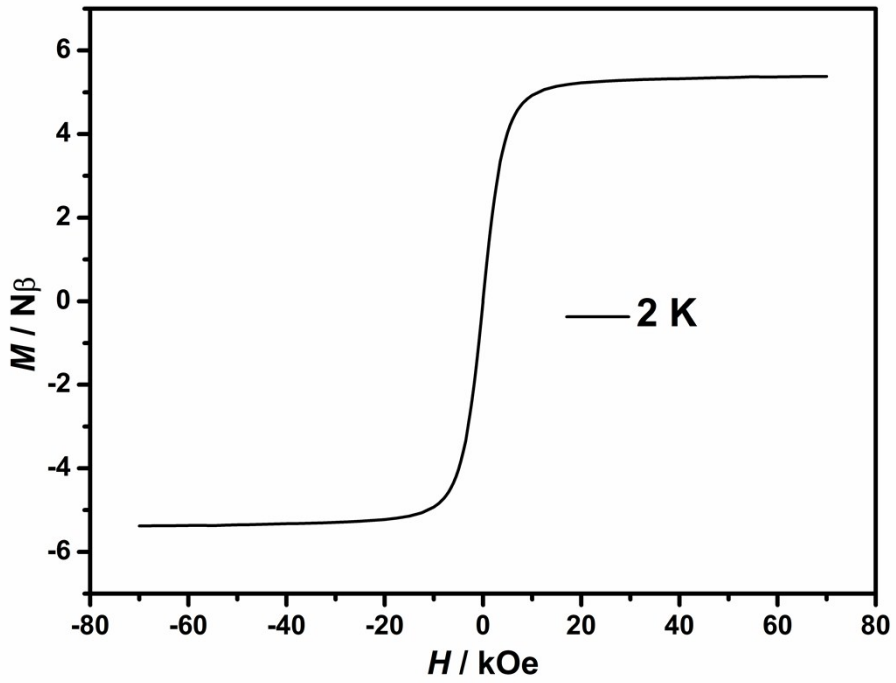

Fig S11. The hysteresis loop with the field sweeping rate of 200 Oe·s^{-1} for **2**.

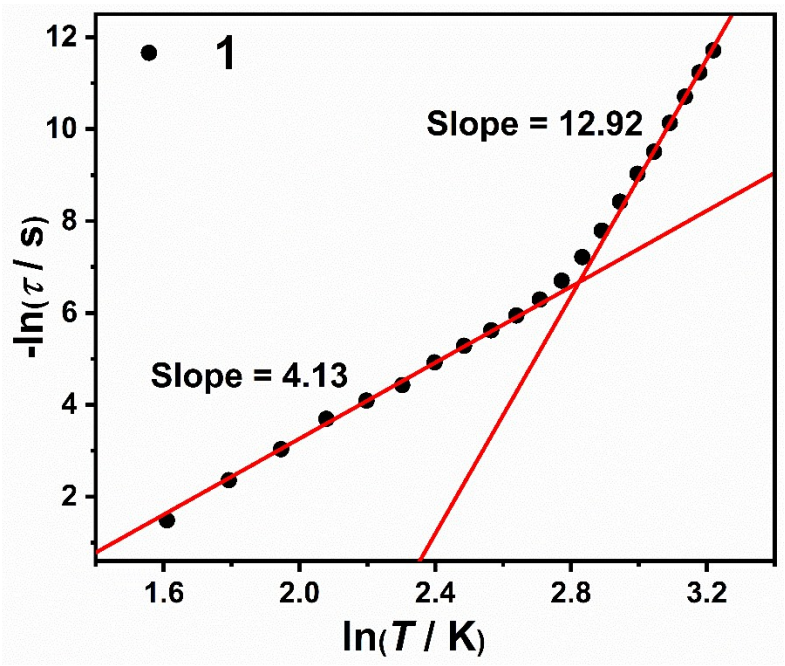

Fig S12. The –lnτ *vs*. ln$T$ plot for **1**. Red lines are linear fitting results.

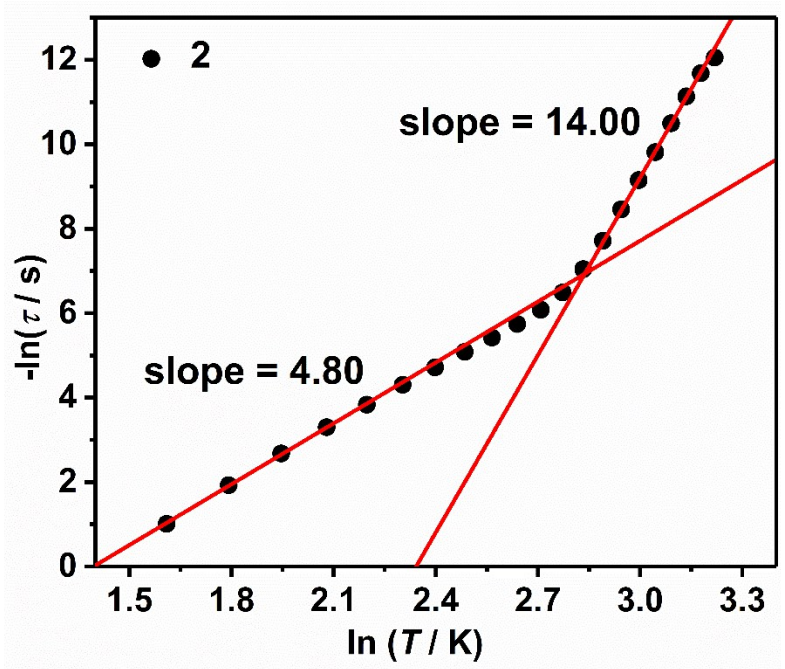

Fig S13. The –lnτ *vs*. ln$T$ plot for **2**. Red lines are linear fitting results.

Table S6. The best fitting parameters for Cole-Cole plots of **1** under zero applied dc field.

T (K)	χ_s	χ_t	τ (s)	α
5	0.67982	6.11662	0.179892	0.22592
6	0.64989	4.57699	0.12329	0.094158
7	0.62345	3.7298	0.09231	0.048
8	0.5923	3.1134	0.08012	0.0248
9	0.55876	2.82883	0.0698378	0.01667
10	0.516676	2.5494	0.0790715	0.0119
11	0.472782	2.31686	0.0752039	0.0072708
12	0.436615	2.12219	0.0724502	0.00505873
13	0.406395	1.96116	0.0696987	0.00361564
14	0.38003	1.82001	0.0634332	0.00261406
15	0.357232	1.69869	0.0545417	0.0018477
16	0.339597	1.59223	0.0398541	0.00122532
17	0.324812	1.49993	0.0235668	7.36397E-4
18	0.327149	1.41398	1.45319E-4	4.13924E-4
19	0.326457	1.34344	9.93965E-5	2.20384E-4
20	0.362656	1.279	7.69567E-5	1.20261E-4
21	0.32189	1.21989	6.89452E-6	7.41741E-5
22	0.29013	1.15978	2.18952E-10	3.96160E-5
23	0.28798	1.11002	3.27882E-10	2.23446E-5
24	0.30129	1.0589	5.23987E-10	1.32191E-5
25	0.31234	1.01497	5.12234E-10	8.15583E-6

Table S7. The best fitting parameters for Cole-Cole plots of **2** under zero applied dc field.

T (K)	χ_s	χ_t	τ (s)	α
5	0.040481	3.90803	0.363049	0.276135
6	0.0435939	2.8149	0.14556	0.219513
7	0.0477184	2.22044	0.0686073	0.167908
8	0.048596	1.86555	0.0369063	0.131677
9	0.0461013	1.6259	0.0215894	0.108885
10	0.0444721	1.44742	0.0134954	0.0933124
11	0.0433054	1.30758	0.00893358	0.0815453
12	0.0424257	1.19398	0.00618559	0.0724974
13	0.041448	1.09877	0.00441274	0.0643409
14	0.0403687	1.01915	0.00320638	0.0579195
15	0.0378835	0.949228	0.00227928	0.0495649
16	0.0364037	0.889757	0.00151661	0.039582
17	0.0239767	0.837218	8.74234E-4	0.0377845
18	0.0138426	0.789709	4.45697E-4	0.0343202
19	0.00353946	0.746947	2.11917E-4	0.0292881
20	0.0209175	0.70881	1.05963E-4	0.010023
21	0.031562	0.67623	5.46445E-5	1.00027E-14
22	4.43096E-16	0.646821	2.75546E-5	2.71468E-14
23	7.17823E-16	0.619519	1.46135E-5	2.83283E-14
24	9.37437E-16	0.593316	8.45066E-6	4.11698E-14
25	1.33679E-15	0.570373	5.81199E-6	5.41421E-14

4. References

[1] (a) H. Zabrodsky, S. Peleg and D. Avnir, *J. Am. Chem. Soc.*, 1992, **114**, 7843; (b) M. Pinsky and D. Avnir, *Inorg. Chem.*, 1998, **37**, 5575.